

## The satellite reversion of dissolved organic carbon (DOC) based on the analysis of the mixing behavior of DOC and colored dissolved organic matter: the East China Sea as an example

LIU Qiong<sup>1,2</sup>, PAN Delu<sup>2\*</sup>, BAI Yan<sup>2</sup>, WU Kai<sup>3</sup>, CHEN Chen-Tung Arthur<sup>4</sup>, SUN Jun<sup>5</sup>, ZHANG Lin<sup>2</sup>

<sup>1</sup> State Key Laboratory for Information Engineering in Surveying, Mapping and Remote Sensing, Wuhan University, Wuhan 430079, China

<sup>2</sup> State Key Laboratory of Satellite Ocean Environment Dynamics, Second Institute of Oceanography, State Oceanic Administration, Hangzhou 310012, China

<sup>3</sup> State Key Laboratory of Marine Environmental Science, College of Oceanography and Environmental Science, Xiamen University, Xiamen 361005, China

<sup>4</sup> Institute of Marine Geology and Chemistry, National Sun Yat-sen University, Kaohsiung, Taiwan, China

<sup>5</sup> College of Marine Science and Engineering, Tianjin University of Science and Technology, Tianjin 300457, China

Received 16 December 2011; accepted 31 May 2012

©The Chinese Society of Oceanography and Springer-Verlag Berlin Heidelberg 2013

### Abstract

The retrieval of dissolved organic carbon (DOC) distribution by remote sensing is mainly based on the empirical relationship of DOC concentration and colored dissolved organic matter (CDOM) concentration in many literatures. To investigate the nature of this relationship, the distributions and mixing behaviors of DOC and CDOM are reviewed in the world's major estuaries and bays. It is found that, generally, the CDOM concentration is well correlated with the salinity in most estuaries, while DOC usually shows a non-conservative behavior which leads to a weak correlation between the DOC concentration and the CDOM concentration. To establish a good satellite reversion of the DOC concentration, the East China Sea (ECS) was taken as an example, and the mixing behavior of DOC and CDOM as well as the influence of biogeochemical processes were analyzed except for the physical mixing process with the data from late autumn (November, 2010) and winter (December, 2009) cruises. In the two ECS cruises, the CDOM concentration was found to be tightly correlated with the salinity, influenced little by the photochemical or biological processes. The data from the winter cruise show that DOC followed a conservative mixing along the salinity gradient, while in the late autumn cruise it was significantly affected by the biological activities, resulting in a poor correlation between the DOC and the CDOM. Accordingly, an improved DOC algorithm (CSDM) was proposed: when the biological influence was significant (Chl  $a$  greater than  $0.8 \mu\text{g}/\text{dm}^3$ ), DOC was retrieved by the conservative and biological model, and if the conservative mixing was dominant (Chl  $a$  less than  $0.8 \mu\text{g}/\text{dm}^3$ ), the direct DOC concentration and CDOM concentration relationship was used. Based on the proposed algorithm, a reasonable DOC distribution for the ECS from satellite was obtained in this study, and the proposed method can be applied to the other large river-dominant marginal sea.

**Key words:** dissolved organic carbon, colored dissolved organic matter, estuary, East China Sea, satellite reversion

**Citation:** Liu Qiong, Pan Delu, Bai Yan, Wu Kai, Chen Chen-Tung Arthur, Sun Jun, Zhang Lin. 2013. The satellite reversion of dissolved organic carbon (DOC) based on the analysis of the mixing behavior of DOC and colored dissolved organic matter: the East China Sea as an example. *Acta Oceanologica Sinica*, 32(2): 1–11, doi: 10.1007/s13131-013-0272-x

### 1 Introduction

Carbon cycle has been an issue of great concern in recent years as the greenhouse gas  $\text{CO}_2$  increased dramatically in the last 200 a. Marine carbon cycle is an important part of the global carbon cycle, which has a significant influence on climate change (Joos et al., 1999). As the largest reservoir of organic carbon in the ocean, dissolved organic carbon (DOC) plays a major role in the carbon cycle and acts as one of the major components of the food webs (Packard et al., 2000). In the ocean it was estimated 685 Gt of organic carbon is in forms of DOC,

equal to the  $\text{CO}_2$  stock in the atmosphere (Hansell and Carlson, 2001). However, DOC data are still far from enough to unveil its variation and influence on carbon cycle. Ship-based DOC measurements, as the main data acquisition approach at present, have the restrictions in space and time; on the other hand, the satellite-based observation has the unique advantage in this aspect. Hence, there is a strong desire to develop remote sensing algorithms of DOC concentration (Del Castillo and Miller, 2008; Mannino et al., 2008). The previous studies have reported the satellite-derive DOC concentration for both inland and ocean

Foundation item: The National Basic Research Program of China (973 Program) under contract No.2009CB421202; the Public Science and Technology Research Funds Projects of Ocean of China under contract No. 200905012; and the National Natural Science Foundation of China under contract Nos 40976110 and 40706061.

\*Corresponding author, E-mail: pandelu@sio.org.cn

waters. Several initial approaches utilized band ratio algorithms of reflectance to retrieve DOC concentration (Arenz et al., 1996; Chen and Shi, 2001; Zhang et al., 2005). The method that directly utilizes the empirical relationships between the DOC concentration and the spectra reflectance has been applied mainly in inland water bodies where the DOC concentration is very high. However, since DOC represents a chemical parameter without optical activity and colored dissolved organic matter (CDOM) was one fraction of dissolved organic matter (DOM) which responded to the spectral signals, the above empirical algorithm is quite limited to certain regions or seasons.

CDOM, as the fraction of DOM that absorbs light in both the ultraviolet (UV) and visible domain (Bricaud et al., 1981), can be retrieved from ocean color data (IOCCG, 2000). The behaviors of DOC and CDOM in estuaries and marginal seas have received considerable attention in recent years (Blough and Del Vecchio, 2002; Cauwet, 2002; Del Vecchio and Blough, 2004). Some studies reported a good linear relationship between the DOC concentration and CDOM absorption coefficient in the marginal sea (Ferrari, 2000; Vodacek et al., 1995), resulting from the conservative mixing of DOC and CDOM along the salinity gradient (Del Vecchio and Blough, 2004; Mantoura and Woodward, 1983). In the Mississippi Estuary, both DOC concentration and CDOM absorption coefficients exhibited a tight linear relationship with the salinity in data from five cruises from 2000 to 2005 (Del Castillo and Miller, 2008). Mannino et al. (2008) retrieved the DOC distribution from the MODIS and SeaWiFS data by using the same algorithm with Del Castillo et al. (2008) in the Middle Atlantic Bight where the DOC and CDOM showed strong but seasonally variable relationships. So, it is known that if there are good correlations between the DOC and CDOM concentration in the coastal oceans with simple DOC sources, the remote sensing algorithm of DOC concentration based on this direct relationship could give reasonably good result. However, the conditions become more complicated in some estuaries and coastal oceans, since the biological activities and other biogeochemical processes would have significant influences on the DOC distribution (Benner and Opsahl, 2001; Gardner and Chen, 2004; Rochelle-Newall and Fisher, 2002). Directly utilizing the relationship between DOC and CDOM is not a good choice in these regions.

Hence, a better understanding of the variations of DOC and CDOM relationship and its major control factors becomes important for the development of the remote sensing algorithm of DOC distribution. In this paper, in order to investigate the nature of DOC/CDOM relationships, we reviewed the mixing behavior of DOC and CDOM in the world major rivers, and the variations of the relationship of DOC/CDOM and the influence of biological activities were analyzed by taking the ECS as an example. An improved DOC concentration remote sensing algorithm which considers both conservative mixing and biological influences was then proposed on the basis of the analysis, and a reasonable DOC distribution in autumn in the ECS was obtained. Finally the deviations of the relationship of DOC/CDOM caused by biogeochemical processes were discussed.

## 2 The mixing behaviors of DOC and CDOM in world major estuaries and adjacent coastal oceans

For a better understanding of the mixing behavior of DOC and CDOM in the estuaries and adjacent marginal seas, some published works about the distribution and the mixing behavior of DOC and CDOM in the world major rivers were reviewed

(Table 1). The linear relationships between biogeochemical parameters and the salinity during freshwater and seawater mixing are widely used to study biogeochemistry in estuaries and adjacent coastal oceans. Generally, the distributions of DOC and CDOM are mainly controlled by the physical process, biological activities and photochemical reactions, etc. These biogeochemical processes disrupt the relationships between the DOC concentration (or CDOM absorption coefficient) and the salinity in different levels, resulting in conservative or nonconservative behaviors of DOC and CDOM. To compare the mixing behaviors of DOC and CDOM in different literatures, we employed the correlation coefficient of relationship between DOC (or CDOM) and the salinity by  $r > 0.8$  as the basis of conservative behavior.

From Table 1, the major rivers in Asia were characterized by lowest DOC concentrations (below  $200 \mu\text{mol}/\text{dm}^3$ ) (Cauwet and Mackenzie, 1993; Chen et al., 2004). The large rivers in North America and South America exhibited higher DOC concentrations (mostly over than  $300 \mu\text{mol}/\text{dm}^3$ ) (Gardner and Chen, 2004; Del Castillo et al., 1999; Hedges et al., 1994). The DOC concentrations in gulfs were also influenced by the terrestrial input. For example, the DOC concentration reached  $500 \mu\text{mol}/\text{dm}^3$  in the Baltic Sea with abundant terrestrial river input (Ferrari et al., 1996). DOC concentrations were at a very low level in China's estuaries compared with other great rivers in the world (Cauwet and Mackenzie, 1993; Chen et al., 2004; He et al., 2010; Lin et al., 2007).

We can also see DOC behaved nonconservatively or quasiservatively in most of estuaries as a result of other biogeochemical processes, like phytoplankton production and microbial degradation. However, it tended to show a conservative mixing behavior when the biological influence was small or the DOM production was balanced by the consumption. For instance, DOC accumulations were observed at the mid-high salinities in both the Mississippi River estuary and the Chesapeake Bay, which suggest that the significant phytoplankton production may force a DOC concentration higher than the theoretical mixing line (Gardner and Chen, 2004; Rochelle-Newall and Fisher, 2002). On the upper reach of the Zhujiang River, the concentration of DOC was obviously below the theoretical line, when the biological parameters showed a strong microbial degradation in the river (Chen et al., 2004). Nevertheless, DOC behaved conservatively in the Changjiang River Estuary with high turbidity and weak biological activity (Guo et al., 2007).

CDOM, the colored portion of DOM, can absorb UV and visible light especially in the UV and blue band. The absorption spectra of CDOM typically decrease with increasing wavelength exponentially  $\{a(\lambda) = a(\lambda_0)\exp[S \times (\lambda_0 - \lambda)]\}$  (Bricaud et al., 1981; Lundgren, 1976). By fitting the spectral curves with the reference band ( $\lambda_0$ ), the parameter of spectral dependence of CDOM absorption spectrum, the  $S$  value can be obtained. Researchers usually deploy the absorption coefficient at reference bands with 355 nm or vicinal band (such as 440 nm, 337 nm) to represent the concentration of CDOM. The shorter band it was used, the higher value it showed to us. The reference bands chosen by literatures for the comparison of the CDOM concentration are illustrated in Table 1.

It was found that CDOM exhibited the same distribution pattern as DOC, and estuaries with high DOC concentration also had large CDOM absorption coefficients. The Mississippi River Estuary and the Swan River Estuary in Australia contained relatively highest DOC concentrations and the CDOM absorp-

**Table 1.** The distribution of DOC and CDOM in major rivers of the world

| Location           | CDOM<br>$a(355)/m^{-1}$ | $S/nm^{-1}$               | DOC/ $\mu mol \cdot dm^{-3}$ | Salinity             | DOC and salinity                |
|--------------------|-------------------------|---------------------------|------------------------------|----------------------|---------------------------------|
| Amazon River       | 0.14–3.12 <sup>1)</sup> | 0.014–0.033 <sup>1)</sup> | 300–400 <sup>2)</sup>        | 0–36.4 <sup>1)</sup> | NA                              |
| Orinoco River      | 0.43–4.17               | 0.012–0.022               | 70–276                       | 19.7–33.7            | NA                              |
| Changjiang River   | 0.10–1.44 <sup>1)</sup> | 0.017–0.020 <sup>1)</sup> | 100–160 <sup>2)</sup>        | 0–32 <sup>1)</sup>   | NA                              |
| Mississippi River  | 0–14 $a(337)$           | NA                        | 50–446                       | 0–37                 | nonconservative                 |
| St. Lawrence River | 0.2–3.8 $a(365)$        | 0.015                     | NA                           | 0–35.5               | NA                              |
| Zhujiang River     | 0.34–1.40               | NA                        | 86–250                       | 0–34.96              | nonconservative                 |
|                    | 0.24–1.93               | 0.013 8–0.018 4           | NA                           | 0–32.49              | NA                              |
| Swan River         | 0.09–10.87<br>$a(440)$  | NA                        | 83.3–1 500.0                 | 3–36                 | nonconservative                 |
| Funka Bay          | 0.022–0.141<br>$a(440)$ | 0.011–0.024               | NA                           | 31.5–33.9            | NA                              |
| Chesapeake Bay     | 0.4–4.6                 | 0.015–0.024               | 60–290                       | 0–33                 | nonconservative                 |
| South Baltic Sea   | 1.2–12 <sup>1)</sup>    | NA                        | 474–616 <sup>1)</sup>        | NA                   | quasiconservative <sup>2)</sup> |
|                    | 1.2–6.5 <sup>1)</sup>   |                           | 267–831 <sup>2)</sup>        |                      | $r=0.78$                        |
| Middle Atlantic    | 0.05–0.9 <sup>1)</sup>  | NA                        | 70–150 <sup>1)</sup>         | 30.2–36.0            | quasiconservative <sup>2)</sup> |
| Bight              | 0–0.3 <sup>2)</sup>     |                           | 75–150 <sup>2)</sup>         |                      |                                 |
| West Florida shelf | 0.05–2.00<br>$a(375)$   | NA                        | 89–305                       | 27.10–36.18          | NA                              |

| Location           | CDOM and salinity          | CDOM and DOC              | Season               | Literature   |
|--------------------|----------------------------|---------------------------|----------------------|--|
| Amazon River       | NA                         | NA                        | winter               | Green and Blough (1994)<br>Hedges et al. (1994)                                |
| Orinoco River      | conservative $r=0.88$      | NA                        | autumn               | Del Castillo et al. (1999)   |
| Changjiang River   | conservative <sup>1)</sup> | correlation <sup>1)</sup> | summer               | Guo et al. (2007) <sup>1)</sup><br>Cauwet and Mackenzie (1993) <sup>2)</sup>   |
| Mississippi River  | conservative               | no correlation            | spring               | Chen and Gardner (2004)  |
| St. Lawrence River | conservative $r>0.95$      | NA                        | summer               | Nieke et al. (1997)  |
| Zhujiang River     | conservative               | no correlation            | summer               | Chen et al. (2004)   |
| Swan River         | conservative $r=0.98$      | NA                        | winter               | Hong et al. (2005)   |
| Funka Bay          | nonconservative            | no correlation            | all                  | Kostoglidis et al. (2005)  |
| Chesapeake Bay     | nonconservative            | NA                        | all                  | Sasaki et al. (2005)   |
| South Baltic Sea   | conservative $r=0.92$      | no correlation            | spring<br>summer     | Rochelle-Newall and<br>Fisher (2002)   |
| Middle Atlantic    | NA                         | correlation <sup>1)</sup> | spring <sup>1)</sup> | Ferrari et al. (1996) <sup>1)</sup>  |
|                    |                            | $r=0.70-0.96$             | autumn <sup>1)</sup> | Kowalczyk et al. (2010) <sup>2)</sup>  |
| Bight              | NA                         | correlation               | summer               | Vodacek et al. (1995) <sup>1)</sup><br>Del Vecchio et al. (2004) <sup>2)</sup> |
| West Florida shelf | NA                         | no correlation            | spring               | Del Castillo et al. (2000)   |

Notes: According to the discharge, the Amazon River, the Orinoco River, the Changjiang River, the Mississippi River, the St. Lawrence River and the Zhujiang River rank 1, 3, 5, 7, 11 and 16 respectively (McKee, 2003), NA denotes no data. The notes 1) and 2) behind data mean the corresponding literature list in the last column.

tion coefficient of freshwater end member was  $14 m^{-1}$  [ $a(355)$ ] and  $10.87 m^{-1}$  [ $a(440)$ ] respectively. On the contrary, the concentrations of CDOM were generally low in China's estuaries, for example, in the Zhujiang River Estuary and the Changjiang River Estuary. The spectral slope value  $S$  depicts how rapidly the absorption decreases with increasing wavelength and provides information about the "nature" of CDOM compositions (Carder et al., 1989; Stedmon and Markager, 2001). The value of  $S$  for CDOM from a wide variety of sources ranged from as low as  $0.01 nm^{-1}$  for terrigenous CDOM to as high as  $0.02-0.03 nm^{-1}$  for oligotrophic seawaters (Blough and Del Vecchio, 2002). In general, the variation of  $S$  is relatively low in the rivers and open oceans; however, there are significant variations in most of the listed estuaries (Table 1), which implies that the CDOM composition probably changed significantly in the mixing processes.

Although the absorption coefficient of CDOM differed in various estuaries and coastal oceans, a conservative mixing be-

havior of CDOM was observed in seven out of nine estuaries and bays in Table 1. This would suggest that the hydrodynamic mixing process dominated the CDOM distribution in estuaries, and the photochemical reaction and biological activity had little effect on the CDOM distribution (Blough and Del Vecchio, 2002). For the other two estuaries and bays without observing the conservative mixing behaviors of CDOM, such as in the Funka Bay, the distribution of CDOM was influenced little by terrestrial input; the primary source of CDOM in these rivers was autochthonous (Sasaki et al., 2005), which leads to a weak correlation between the CDOM concentration and the salinity.

From the above descriptions, it can be concluded that CDOM usually follows a conservative mixing behavior in most estuaries and bays, while DOC is often significantly influenced by biological activities and follows a nonconservative mixing. As we know, a close relation between CDOM concentration and DOC concentration is the basis of the CDOM-based algorithm.

m. In the listed literatures in Table 1, there are three river estuaries with significant correlations between CDOM and DOC in a total of eight river estuaries where observations were available. In other five river estuaries such as the Zhujiang River, Mississippi River Estuaries, the weak correlations between CDOM concentration and DOC concentration would prevent accurate estimations of DOC concentration from CDOM product. In our paper, we would mainly focus on such areas and make a deep discussion on DOC remote sensing under the condition that a significant relationship between DOC and CDOM is not observed, in order to develop an improved DOC remote sensing algorithm, we took the East China Sea (mainly influenced by the Changjiang River) as the study region and analyzed the physical and biological influences on the relationship between DOC and CDOM.

As discussed in the above sections, the primary method of DOC remote sensing is to utilize the CDOM absorption coefficient as a proxy to retrieve the concentration of DOC based on the empirical relationship of CDOM and DOC (Del Castillo and Miller, 2008; Mannino et al., 2008). It should be noted that good inversion results require a stable relationship of DOC and CDOM, but in coastal oceans with complex biogeochemical conditions the performance of the method was not satisfactory.

### 3 Estimation of DOC concentration by remote sensing in the ECS

In this section by taking the ECS as an example, we analyzed the mixing behaviors of DOC and CDOM, and the signif-

icant influence of biogeochemical processes on the empirical relationship. Then the CSDM algorithm which considered the discussions on control factors of DOC/CDOM relationship was established by analyzing the late autumn and winter cruise data, finally the proposed model was applied to obtain the DOC distribution of the ECS in winter.

#### 3.1 DOC remote sensing in the ECS

##### 3.1.1 Data and methods

Two cruises (CHOICE-C cruises, “973” Project”) were conducted in ECS, one in December 2009, and the other in November 2010, covering most shelf areas of the ECS (Fig. 1). Niskin bottles were used in sampling to avoid contamination. The DOC and CDOM sampling followed the JGOFS protocols (Knap, 1996) and the NASA relative sampling principle (Mitchell et al., 2000), respectively. The DOC samples were filtered on board through the Whatman GF/F glass fiber filters ( $0.7 \mu\text{m}$  pore size), and the CDOM samples were filtered through the Gelman fluted capsule filter ( $0.2 \mu\text{m}$  pore size). Both DOC and CDOM samples were stored in the dark at  $-20^\circ\text{C}$  until measurements. The chlorophyll a samples were collected by filtrating seawater through  $\varphi 25 \text{ mm}$  Whatman™ GF/F glass fiber filters, then wrapped the filters in a pieces of aluminum foil and stored in a  $-20^\circ\text{C}$  refrigerator before analysis.

The DOC samples were analyzed by the TOC- $V_{\text{CPH}}$  (Shimadzu) analyzer, utilizing the high temperature combustion method which combusts the DOC of water samples into  $\text{CO}_2$  and then detects the produced  $\text{CO}_2$  by a non-dispersive Infrared sensor. The details of DOC concentration measurements were

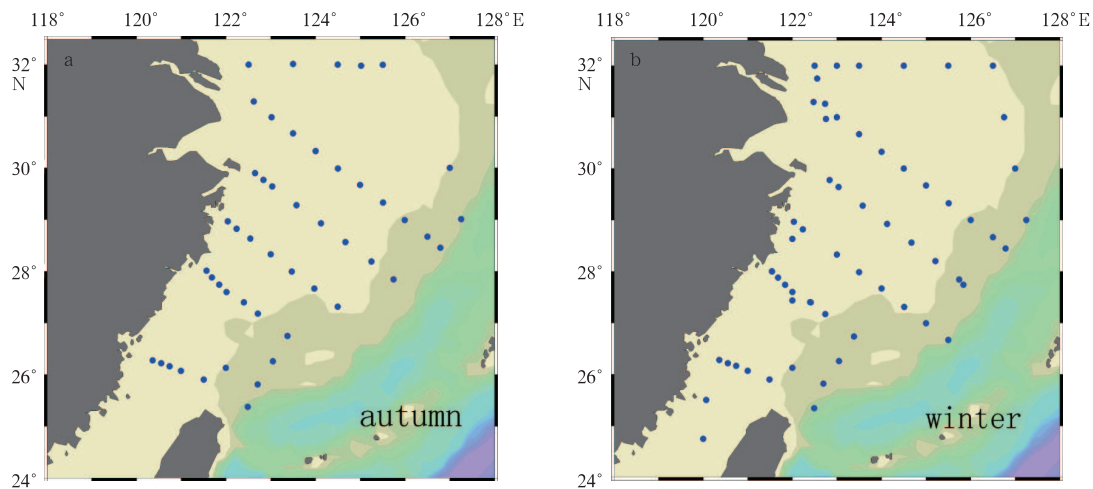


**Fig. 1.** The sampling stations of autumn and winter cruise in East China Sea. a. The autumn cruise in November 2010 and b. the winter cruise in January 2010.

described in Dai et al. (2009). CDOM samples were analyzed by the PE Lambda35 spectrometer using the light transmission measurement methods. The samples were scanned (300–900 nm) with spectral resolution of 1nm. The details of CDOM concentration measurements were described in Lei et al. (2012). The chlorophyll was extracted in the dark with 90% acetone for 24 h at  $-20^\circ\text{C}$  before analysis, and was measured by a Turner-Designs fluorometer *Trilogy*™ using the nonacidification fluorometric method (Welschmeyer, 1994).

##### 3.1.2 The distribution and the mixing behavior of DOC and CDOM

We show the relationships [ $c(\text{DOC})$ ,  $c(\text{CDOM})$ ] of DOC

and CDOM concentration with salinity in Fig. 2 in the late autumn cruise (November 2010) and winter cruise (December 2009), and the chlorophyll a concentrations were presented by the color of the dots. Generally, the concentrations of DOC and CDOM in the surface layer of the ECS showed the similar pattern, decreasing from the nearshore to the shelf in these two seasons. However, in winter, the concentrations of DOC and CDOM were higher in nearshore than that in the later autumn. In the bloom areas the CDOM absorption coefficients almost double, and correspond to the high DOC concentration.

As indicated by Fig. 2, the chlorophyll a distributions were totally different between the data from the late autumn cruise

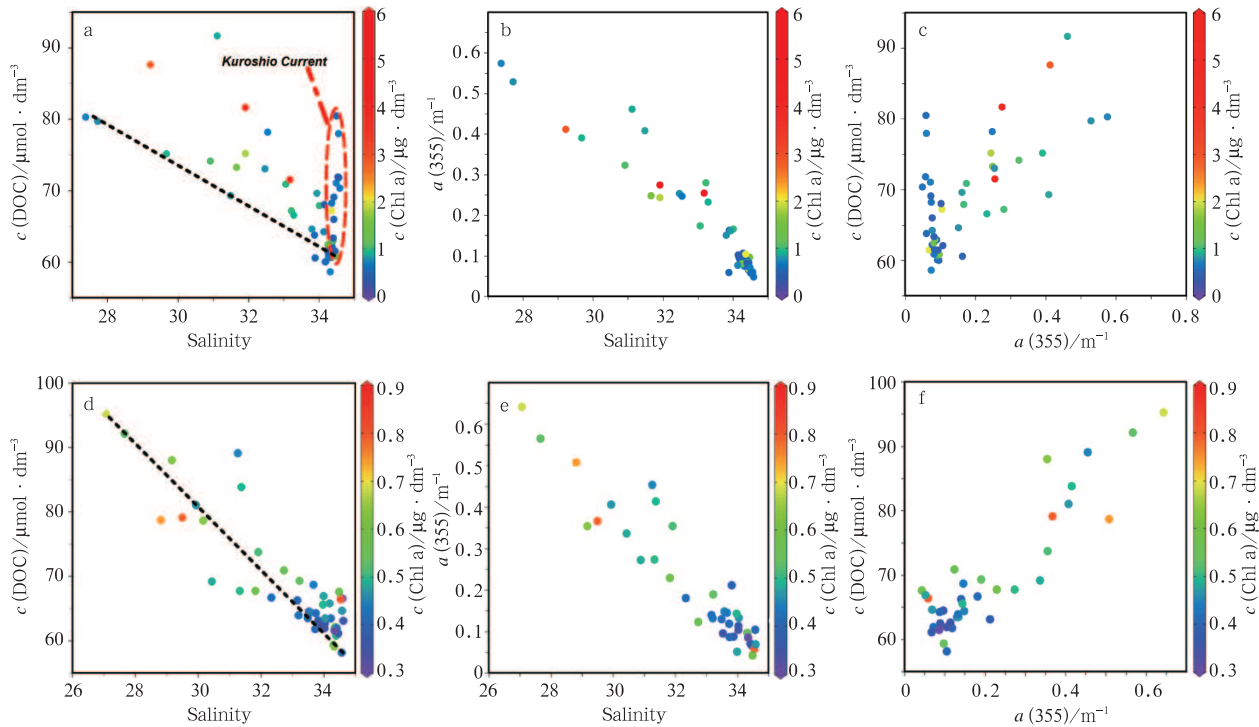


**Fig. 2.** In the late autumn cruise the relationships between DOC and salinity (a), CDOM and salinity (b), DOC and CDOM (c); and in the winter cruise the relationships between DOC and salinity (d), CDOM and salinity (e), DOC and CDOM (d). The Chl a concentration are represented by the color of scattered dots. The dashed lines in Figs 2a and d were the physical mixing line of between end members.

and winter cruise. In the late autumn, the concentrations of chlorophyll a ranged from  $0.340\ 0\ \mu\text{g}/\text{dm}^3$  to  $6.357\ 7\ \mu\text{g}/\text{dm}^3$ , and the average value was about  $1.21\ \mu\text{g}/\text{dm}^3$ . In the winter it ranged from  $0.280\ \mu\text{g}/\text{dm}^3$  to  $0.806\ \mu\text{g}/\text{dm}^3$ , the average concentration was  $0.48\ \mu\text{g}/\text{dm}^3$ , much lower than the autumn distribution.

From Fig. 2 it can be inferred that the DOC concentration from the winter cruise showed little variation and a good correlation with the salinity ( $r^2 = 0.806$ ,  $P < 0.001$ ); the absorption coefficients of CDOM also exhibited a conservative behavior as a result of physical mixing, and so a fairly good relationship between DOC and CDOM was observed in the winter data ( $r^2 = 0.816\ 4$ ,  $P < 0.001$ ). However, the relationship between DOC and salinity in the late autumn cruise was not good as that in winter, it behaved quasi conservatively. Also the data points which stay above the physical mixing line (described in below section) were often characterized by high chlorophyll a concentrations (Fig. 2a). However, CDOM correlated well with salinity in the late autumn. As a result, the DOC concentration and the CDOM concentration were not significantly correlated ( $r^2 = 0.466\ 4$ ,  $P < 0.001$ ). In most of shelf areas the DOC distribution is a result of mixing of terrestrial freshwater with the high DOC concentration and shelf seawater with the low DOC concentration, however, the outer shelf and offshore regions in the ECS were dominated by the Kuroshio Current characterized by high salinity and temperature, a totally different DOC source (Hung et al., 2003). Hence, the data from the late autumn cruise contained a great variety of DOC at the high salinities (Fig. 2a). The DOC concentration ranged from  $60\ \mu\text{mol}/\text{dm}^3$  to  $80\ \mu\text{mol}/\text{dm}^3$  when the salinity was above 34.0. Excluding the data from the

outer shelf and continental slope region sites (shown in Fig. 2), the relationship between DOC and CDOM became significant ( $r^2 = 0.7$ ,  $P < 0.001$ ), it indicated that the DOC distribution was mainly controlled by physical mixing in this season. However, the DOC/CDOM relationship from the late autumn cruise was still not significant when compared with the winter data ( $r^2 > 0.8$ ), as the DOC distribution was notably influenced by the other biogeochemical process.

The DOC/CDOM relationships in the data from the cruises in the ECS were remarkably different. In winter DOC exhibited a conservative behavior in the mixing process, which indicated that the DOC distribution was affected by the physical mixing process and influenced little by the biological activities. However, in late autumn the DOC/CDOM relationship was very scattered, as the DOC distribution was significantly influenced by the biological activities besides the physical mixing. Consequently, for the purpose of improving the relationship between DOC and CDOM in autumn cruise, the biological effects should be considered.

### 3.1.3 The DOC remote sensing model

The above analysis indicates that, the empirical relationship between DOC and CDOM concentration used in the algorithm of DOC remote sensing, can be treated as the conservative mixing model (conservative model) of DOC. This model is suitable for the cases when CDOM and DOC are both conservatively mixing in the estuaries and coastal oceans, as demonstrated in the Middle Atlantic Bight (Mannino et al., 2008). Here we also established the conservative model for both two ECS cruise (the data of Kuroshio Current water were excluded), the models are as follows:

$$\left. \begin{aligned} c(\text{DOC}) &= 45.711a(\text{CDOM}, 355) + 58.914 \\ (r^2 &= 0.7, P < 0.0001 \text{ in late autumn}), \\ c(\text{DOC}) &= 53.355a(\text{CDOM}, 355) + 58.609 \\ (r^2 &= 0.795, P < 0.0001 \text{ in winter}). \end{aligned} \right\} \quad (1)$$

The above conservative models suggest that the winter cruise data exhibit a more significant DOC/CDOM relationship, the data from the late autumn cruise show more scattered relationship due to the influence of biological processes. In order to illustrate the biological influence over the empirical relationship, we divided the changes of the observed DOC concentration along the salinity gradient into two parts: the changes caused by the physical linear mixing and the biological impacts. The later part can be demonstrated by subtracting the DOC concentration estimated from the theoretical physical mixing line from the observed DOC concentration value; here we named this item  $\Delta c(\text{DOC})$ .

$$\left. \begin{aligned} \Delta c(\text{DOC}) &= c_o(\text{DOC}) - c_{t1}(\text{DOC}) \\ c_{t1}(\text{DOC}) &= (S_o - S_{\min})[c_{re}(\text{DOC}) - c_{se}(\text{DOC})] / (S_{\max} - S_{\min}) \end{aligned} \right\}, \quad (2)$$

where  $c_o(\text{DOC})$  represents the observed DOC concentration;  $c_{t1}(\text{DOC})$  is the DOC concentration of theoretical linear mixing between two end members (the freshwater end and the seawater end);  $S_o$  is the observed salinity;  $S_{\min}$  and  $S_{\max}$  are the mini-

um and maximum salinities in the observed data, which represent the freshwater and seawater respectively; and  $c_{re}(\text{DOC})$  and  $c_{se}(\text{DOC})$  are the DOC concentrations in corresponding  $S_{\min}$  and  $S_{\max}$ . The end members were determined by using the maximum and minimum salinities, which may be sort of subjective as the variability of end members was recognized as a confusing problem (Rochelle-Newall and Fisher, 2002). Nevertheless, the minor error caused by the determination of the end members would have little impact to our conclusion below.

Obviously the relationship between Chl a concentration and the  $\Delta c(\text{DOC})$  in winter was not significant at all ( $r=0.2$ ,  $P > 0.05$ , Fig. 3a). It should be noticed that the Chl a concentrations were under  $0.8 \mu\text{g}/\text{dm}^3$  for almost all data points, which suggested that the phytoplankton production was weak and had little impact on the DOC distribution in winter, and the physical mixing process has a dominant influence on the DOC distribution. However, the Chl a concentration was relatively high (about half part of stations above  $1 \mu\text{g}/\text{dm}^3$ ) in most of the stations in the late autumn cruise, and it was notably correlated with the  $\Delta c(\text{DOC})$  (Fig. 3b), indicating that the  $\Delta c(\text{DOC})$  mainly comes from the phytoplankton production. This significance between the Chl a concentration and  $\Delta c(\text{DOC})$  also explained the scatter of DOC/CDOM relationship in the late autumn cruise, which was consistent with the observation in many estuaries and adjacent coastal oceans (Benner and Opsahl, 2001; Rochelle-Newall and Fisher, 2002): the phytoplankton production was the most important biological process during mixing.

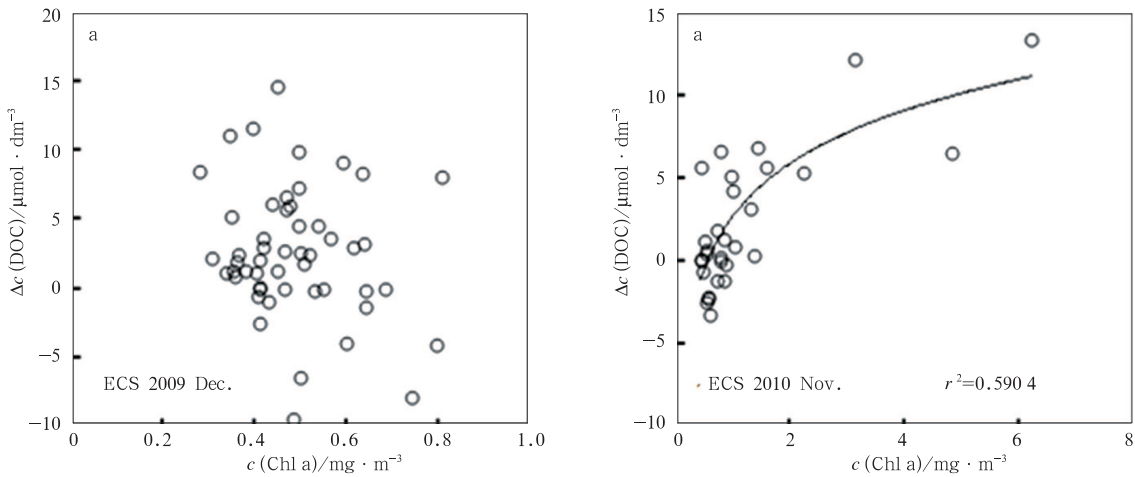


**Fig.3.** The relationship between  $\Delta c(\text{DOC})$  and  $c(\text{Chl a})$  in winter 2009 cruise (a) and in late autumn 2010 cruise (b).

To improve the accuracy of the conservative model in the autumn cruise, we employed the Chl a concentration to represent the biological activities and estimate the biological influences. The linear relationship between DOC and CDOM was regarded as the conservative model for DOC; meanwhile we used these three parameters to run multiple linear regressions and established the conservative and biological model (CBM) for DOC:

$$c(\text{DOC}) = Aa(\text{CDOM}, 355) + Bc(\text{Chl a}) + C. \quad (3)$$

Therefore, we used the data in late autumn cruise which contains the DOC, CDOM and Chl a parameters to establish the

CBM model (Eq. 3); meanwhile, we used the conservative model which only has one parameter of CDOM (Eq. 4) for comparison:

$$\left. \begin{aligned} c(\text{DOC}) &= 43.076a(\text{CDOM}, 355) + 59.284 \\ (r^2 &= 0.7, d_{st} = 3.9 \mu\text{mol}/\text{dm}^3), \\ c(\text{DOC}) &= 39.965a(\text{CDOM}, 355) + \\ &\quad 1.733c(\text{Chl a}) + 57.956 \\ (r^2 &= 0.748, d_{st} = 3.6612 \mu\text{mol}/\text{dm}^3). \end{aligned} \right\}. \quad (4)$$

The above equations indicate that the CBM obtains a better fit of the cruise data than the conservative model in late autumn, with higher  $r$  square and smaller stand deviation.

The data in winter cruise were utilized for validating the

accuracy and adaptability of the above two models, and the statistical results are shown in Table 2. The mean APD (absolute percent difference) was the ratio of difference between the modeled result and the field observation to the field observation. In the situation of winter, both of the CBM and conservative model can return good results, but the results of the conservative model show slightly higher accuracy than the CBM result, which can be attributed to the weak correlation between  $\Delta c(\text{DOC})$  and Chl a concentration (by Fig. 3a).

**Table 2.** The error analysis for the CBM and the Conservative model, the winter cruise data (December, 2009) were employed for validation

| Method             | Mean APD(%) | RMSE/ $\mu\text{mol}\cdot\text{dm}^{-3}$ | $r^2$ |
|--------------------|-------------|--|-------|
| CBM                | 5.732       | 6.078                                    | 0.687 |
| Conservative model | 5.446       | 5.523                                    | 0.683 |

Therefore, the conservative model is more fit to the winter cruise data and the CBM is suitable for the late autumn cruise data. We noticed that in winter cruise the Chl a concentrations

were much lower than in the late autumn cruise; nearly all data points are lower than  $0.8 \mu\text{g}/\text{dm}^3$ . The two cruises show great disparity on the ranges of Chl a concentration, hence, this basic biological parameter could be used to determine whether the DOC concentration is significantly affected by the biological activity or not.

By integrating the data from both two cruises, it was found that the phytoplankton production has a significant influence on the DOC distribution when the Chl a concentration is above  $0.8 \mu\text{g}/\text{dm}^3$ , the  $\Delta c(\text{DOC})$  is well correlated with the Chl a concentration. On the contrary, DOC concentration is tightly correlated with salinity and the biological influence tends to be negligible when the Chl a concentration is below  $0.8 \mu\text{g}/\text{dm}^3$ . Ogawa et al. (2003) also demonstrated that the DOC was influenced little by the Chl a distribution (below  $0.7 \mu\text{g}/\text{dm}^3$ ) in the northern ECS. Based on these findings, the water can be separated into two types of situation according to the Chl a concentration: CBM can be applied to the water with high Chl a concentration, and the conservative model can be applied to the water with low Chl a. We can obtain the Chl a-based synthetic DOC model (CSDM) as the diagram in Fig. 4.

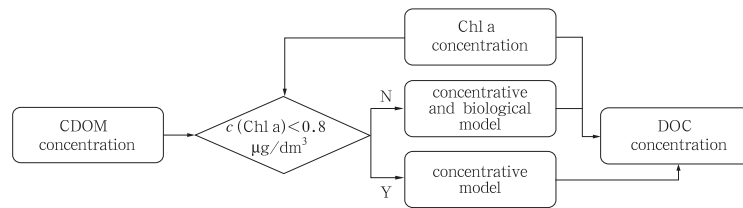


**Fig.4.** The synthetic DOC model based on the Chl a threshold (CSDM).

The late autumn and winter cruise data were served as input to establish the above DOC reversion model [Eq. (5)]

$$\left. \begin{aligned} c(\text{DOC}) &= 58.636 + 48.554a(\text{CDOM}, 355) \\ (r^2 &= 0.79), \\ c(\text{DOC}) &= 58.114 + 2.260c(\text{Chl a}) + \\ &41.212a(\text{CDOM}, 355) \\ (r^2 &= 0.774). \end{aligned} \right\} \quad (5)$$

The CSDM gives a better fit to the field data than the conservative model and CBM. Neither type of water has a better accuracy with  $r$  square closed to 0.8. Hence, by using this model we could obtain a better reversion result of DOC concentration from the satellite.

#### 3.1.4 Satellite-derived DOC mapping and validation

As the daily and 8 d averaged satellite products are covered by cloud in most of the areas of the ECS, we downloaded the SeaWiFS products of monthly averaged water leaving radiance at six bands with spatial resolution of 9 km from NASA ocean color website. Then we used a newly developed model of extended QAA (QAA-E) developed by Zhu et al. (2011) to get the satellite-derived CDOM images. Zhu et al. QAA-E model can separate  $a(\text{CDOM})$  from QAA-derived  $a(\text{CDM})$  (the combined absorption coefficient of CDOM and detritus). The detail of the QAA-E algorithm can be referred in the paper of Zhu et al. (2011).

We obtained the autumn distribution of DOC in the ECS. The reversion of DOC concentration resulted from both the

conservative model and CSDM showed a very similar distribution pattern in autumn (Figs 5a and b). The difference of the two models was mainly laid in the near-shore areas where high Chl a concentration was observed, and there was almost no difference between two models in the middle and outer shelf regions. Meanwhile, the high concentrations of CDOM would weaken the influence of Chl a concentration (Eq. 5), resulting in a similar DOC distribution between the CSDM and conservative model.

As compared with the field measured DOC data (the late autumn cruise), both two models overestimated the DOC concentration for about  $5\text{--}15 \mu\text{mol}/\text{dm}^3$  in the middle ECS shelf areas. This is caused by the existence of high concentration of non-algal particle (NAP) in the ECS and the resulting overestimation of CDOM. The especially high DOC concentrations in the regions outside the Changjiang River Estuary were attributed to an algal bloom, which was observed in the cruise. In outer shelf areas, the DOC concentrations are consistently low compared with CDOM distribution, which is also underestimated when compared with the in situ data. This disparity is restricted by the CDOM-based algorithm which utilizes two end-members mixing model.

Hung et al. (2003) investigated the DOC distribution of four seasons in the ECS from 1996 to 1998, and found that the DOC concentrations were ranged from  $85 \mu\text{mol}/\text{dm}^3$  to  $120 \mu\text{mol}/\text{dm}^3$  in coastal areas, from  $72 \mu\text{mol}/\text{dm}^3$  to  $85 \mu\text{mol}/\text{dm}^3$  in shelf mixed areas and from  $75 \mu\text{mol}/\text{dm}^3$  to  $85 \mu\text{mol}/\text{dm}^3$  in the Kuroshio Water. Our satellite-derived results (Figs 5c and d)

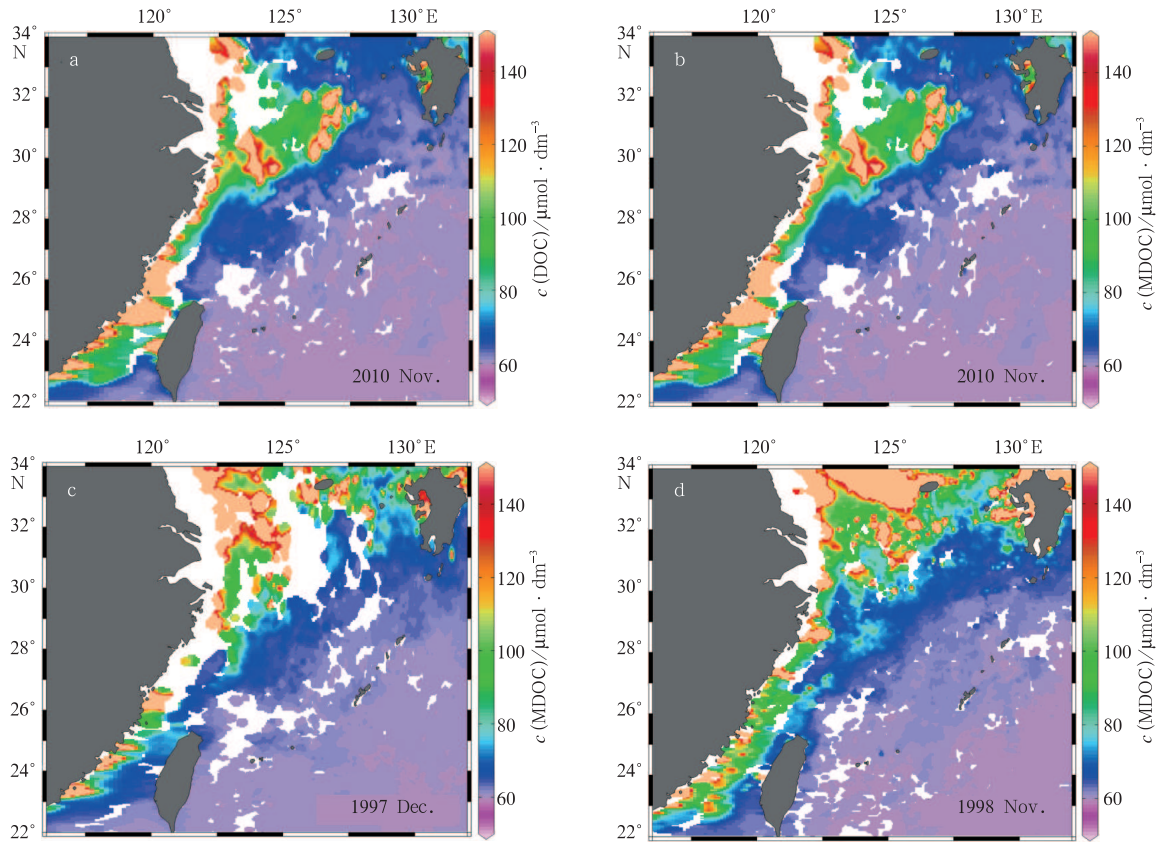


**Fig. 5.** The satellite images are the reversion result of DOC concentration from the conservative model in the autumn of 2010 (a), the CSDM in the autumn of 2010 (b), the CSDM in the winter of 1997 (c) and the CSDM in the autumn of 1998 (d).

are at the same magnitude level compared with the DOC distributions from Hung et al. (2003) in the continental shelf areas, and the distribution pattern is much similar to each other in autumn in shelf regions.

Overall, the reversion results of the two models just differed from each other in the coastal areas where the DOC concentrations were observed above the theoretical mixing line due to the significant phytoplankton production. In regions where high CDOM absorption coefficients are observed, the two models gave much the same results as shown in Figs 5a and b. However, the two ECS cruise data showed that the CSDM was closer to the field observations. In the middle and outer shelf areas the two reversion results were about the same. The error of reversion mainly originates from the overestimation of CDOM. Owing to the existence of non-algae particles, which shows very similar spectral characteristics with CDOM, the present algorithms usually overestimated the absorption coefficient of CDOM in coastal areas. Consequently, apart from the further research of the DOC reversion model, the remote sensing algorithm of CDOM also needs to be improved in coastal oceans for DOC remote sensing.

### 3.2 Discussion

#### 3.2.1 The influence of CDOM algorithm

The QAA-E algorithm we employed in retrieving CDOM concentration from satellite is capable of separating the  $a_g$  (CDOM) from the  $a_{dg}$  (the absorption of colored detritus matter) (Zhu et al., 2011). The algorithm was verified in the Mississippi

and Atchafalaya River plumes and the Gulf of Mexico, showed a reasonable inversion result for both Case 1 and Case 2 waters. Similarly, the ECS is largely influenced by the Changjiang River plume and includes both Case 1 and Case 2 waters. The data from the autumn cruise were utilized to test the applicability and accuracy of the algorithm when applied in the ECS.

The in situ CDOM absorption measurements and the satellite-derived results are significantly correlated ( $r=0.55$ , RMSE equals 0.38,  $P < 0.001$ ) in the ECS. The APD between the two data sets ranged from 4% to 949%, the mean value was 194.9%, and about 53% stations were under 100% (APD). Unlike the Mississippi River plume and the Gulf of Mexico, CDOM absorption was overestimated in most of the stations, which may be attributed to the different compositions of color detritus matter between the two regions. The inversion accuracy were reasonable and reliable (APD is less than 100%) in the middle and southern shelf areas, while in the northern ECS dominated by Changjiang diluted water, the APD was up to 400%, as there is abundant NAP existing in the seawater which caused big variations in CDOM algorithm. Hence, the QAA-E algorithm is suitable for the most of ECS shelf areas. According to Eq. (5), the mean error of the DOC concentration induced by CDOM algorithm is about  $9.2 \mu\text{mol}/\text{dm}^3$ , constitutes a big part of DOC inversion errors.

#### 3.2.2 The variation of linear relationship between DOC and CDOM

The linear relationship between DOC and CDOM is the important basis to retrieve DOC distribution from the satellite



data, which is affected by the distributions of DOC and CDOM, and various biogeochemical processes related to DOC and CDOM. In the case of the ECS in late autumn and winter, given the consistent CDOM distribution, the DOC concentration in outer shelf regions determines the intercept of the linear equation; and the difference between the DOC concentration in near-shore and outer shelf regions controls the slope of the linear equation. The comparison between the late autumn data and the winter data showed that the CDOM distribution of the ECS was similar in the two seasons, and the DOC concentrations were also close to each other ( $60\text{--}64\ \mu\text{mol}/\text{dm}^3$ ) in outer shelf regions which resulted in a similar intercept ( $\approx 59\ \mu\text{mol}/\text{dm}^3$ ) of the linear relationship between DOC and CDOM. However, the DOC concentrations in near-shore regions were somewhat higher in winter cruise, which leads to a steeper slope in the winter cruise (slope is 51.7) than in late autumn cruise (slope is 43). This seasonal difference implies that a common DOC algorithm in different seasons is impossible, so we developed DOC models for the autumn and winter respectively.

Apart from the physical process, the distributions of DOC and CDOM were affected by various biogeochemical processes. For instance, in the areas of mid-high salinity domain in estuaries, DOC often accumulated in the surface layer and departed from the conservative mixing line due to the phytoplankton production (Benner and Opsahl, 2001), however, new CDOM was generally produced from the microbial and bacteria production rather than the phytoplankton production (Nelson et al., 1998). Accordingly the biogeochemical processes which have impact on the distribution of DOC and CDOM were totally different in the estuaries and the adjacent coastal oceans. As a result the relationships between DOC and CDOM always exhibited a nonlinear relationship (Chen and Gardner, 2004). DOC would correlate well with CDOM only under the condition that the physical mixing process has a dominant influence on their distributions and the biogeochemical processes can be neglected.

### 3.2.3 Deviations of the DOC mixing behavior

In late autumn in ECS, the relationship between DOC concentration and the salinity was not as significant as CDOM concentration and salinity according to Fig. 2a. The DOC distribution was influenced notably by other biogeochemical processes than the physical mixing process. Generally, the sources of DOC could be divided into autochthonous and external sources. The terrestrial input was the major external source of DOC in estuaries and adjacent coastal oceans, and the phytoplankton production, sloppy feeding, virus lysis processes were important autochthonous sources of DOC (Carlson, 2002). DOC was removed mostly via the consumption of heterotrophic bacteria which utilized the DOC as their food sources (Nagata, 2002).

DOC can be secreted by phytoplankton during the photosynthesis process. The transparency of water body was usually low in estuaries due to the large number of suspended solid matter brought by river and intense resuspension. As a result the phytoplankton production would be limited. In the areas with mid-high salinity (15–35), the water transparency turned higher because the bulk of suspended solids had settled down and the resuspension weakened (Benner and Opsahl, 2001); meanwhile, the plentiful nutrients brought by the river facilitated the phytoplankton production and then the maximum phytoplankton production often occurred at these mid-high salinity areas (Chen and Gardner, 2004; Lohrenz et al., 1990; Lohrenz

et al., 1999). Many studies have also found that the DOC concentration in areas of mid-high salinity were significantly higher than the conservative mixing line caused by phytoplankton production. For example, in the autumn of 1997, Rochelle-Newall and Fisher (2002) observed an evident accumulation of DOC with the increase of Chl *a* concentration at mid-high salinities in the Chesapeake Bay; also a remarkable influence on the distribution of DOC by the phytoplankton production was found by Benner and Opsahl (2001), especially in the summer of 1990 and 1993, almost all of the DOC concentration were above the conservative mixing line at mid-high salinities.

Our usage of  $\Delta c(\text{DOC})$  can estimate the biological effect on DOC above the basic physical mixing. The important relationship between  $\Delta c(\text{DOC})$  and  $c(\text{Chl } a)$  in autumn in ECS suggests that the DOC distribution was influenced by the phytoplankton production (Fig. 3b). Hence, on the basis of the observation in late autumn and other similar observations, the accumulations of DOC were considered to be the combined results of DOM autochthonous sources and sinks in our DOC remote sensing model, and the phytoplankton production (represented by the Chl *a* concentration) is considered responsible for the DOC accumulations.

Besides, the DOC accumulations during the physical mixing were not just the result of phytoplankton production; microbial consumption, sloppy feeding, virus lysis and many other biological processes also had impacts on the DOC distribution. These processes then decreased the stability of significant relation between  $c(\text{Chl } a)$  and  $\Delta c(\text{DOC})$ , and produced notable deviation when using Chl *a* to represent the biological influences. However, these processes and parameters could not be approached via remote sensing by now. The further improvement of DOC concentration reversion will rely on the future development of the bio-optical remote sensing algorithm. In different seasons and regions, different phytoplankton species may result in different relationships between  $c(\text{Chl } a)$  and  $\Delta c(\text{DOC})$ . A consideration of the changes of phytoplankton species in different seasons and regions would improve the CSDM.

## 4 Conclusions

The development of remote sensing algorithms of DOC is vital for us to understand the distribution and variety of marine organic carbon reservoirs. In estuaries and adjacent marginal seas, freshwater with the high concentrations of DOC and CDOM is blended with seawater with low concentrations; generally it led to consistent changes of the magnitudes of DOC and CDOM concentration along with the salinity. Consequently, obtaining the DOC distribution via the empirical relationships between DOC and CDOM became the principal way of DOC remote sensing in coastal oceans.

Based on the method of DOC concentration estimation by remote sensing, in this paper we collected and analyzed the information about the distributions and mixing behaviors of CDOM and DOC in the world major estuaries and adjacent marginal oceans. With the mechanisms analysis, we proposed the CSDM algorithm: for the regions where the biological influence is significant [ $c(\text{Chl } a) > 0.8\ \mu\text{g}/\text{dm}^3$ ] the DOC distribution can be acquired by conservative and biological model, and for the regions where biological activities are weak with the concentration of Chl *a* below  $0.8\ \mu\text{g}/\text{dm}^3$ , conservative model is applied. Then the data from the late autumn and winter cruise

in the ECS were used to establish the DOC remote sensing model in dry seasons. Finally, a reasonable DOC distribution in the ECS in autumn was obtained from the satellite derived CDOM and Chl *a* images: the satellite-derived result has a quite similar distribution pattern in almost shelf areas, and is about 5–15  $\mu\text{mol}/\text{dm}^3$  higher than the cruise data which mainly comes from the error of satellite-derived CDOM product. The comparison of satellite-derived results and in situ data from Hung et al. (2003) also demonstrates a good estimation from the improved algorithm.

At present, estimating DOC distribution from the satellite CDOM concentration data is the primary and practical way. The traditional conservative model is more suitable for the regions without significant biological influences; in this paper we demonstrate that the conservative and biological model was able to achieve the improved results in coastal oceans with notable biological influences. The combination of the two models based on Chl *a* concentration makes the CDOM-based algorithm suitable for ECS areas in dry seasons, whether significantly influenced by biological activities or not. By integrating in situ measurements, the CSDM is able to be applied in most of coastal oceans in different seasons. However, the algorithm still has its limitations. More data are needed to understand the variability of terrestrial input in different seasons, which can lead to a change of the conservative relationship. The question that how to estimate the seasonal change of the conservative relationship and the variety of DOC production induced by diverse phytoplankton species should be addressed in the future research. Furthermore, the accuracy of satellite-derived CDOM products is severely affected by the existence of abundant NAP in turbid waters. The improvement in the CDOM remote sensing algorithm in these regions is also important for the remote sensing of DOC concentration.

#### Acknowledgements

The authors would like to thank the NASA for providing the satellite data. Qian Wei, Meng Feifei and Chen Junhui are thanked for their assistance in the DOC sampling and analysis. And thanks to Professor Dai Minhan for the valuable suggestions and Charles Chi-Li Tang for the great help in the English.

#### References

- Arenz R, Lewis W, Saunders J. 1996. Determination of chlorophyll and dissolved organic carbon from reflectance data for Colorado reservoirs. *International Journal of Remote Sensing*, 17(8): 1547–1565
- Benner Ronald, Opsahl Stephen. 2001. Molecular indicators of the sources and transformations of dissolved organic matter in the Mississippi River plume. *Organic Geochemistry*, 32(4): 597–611
- Blough Neil V, Del Vecchio Rossana. 2002. Chromophoric DOM in the coastal environment. In: Dennis A H, Craig A C, eds. *Biogeochemistry of Marine Dissolved Organic Matter*. San Diego: Academic Press, 509–546
- Bricaud Annick, Morel Andre, Prieur Louis. 1981. Absorption by dissolved organic matter of the sea (yellow substance) in the UV and visible domains. *Limnol Oceanogr*, 26(1): 43–53
- Carder Kendall L, Steward Robert G, Harvey George R, et al. 1989. Marine humic and fulvic acids: their effects on remote sensing of ocean chlorophyll. *Limnol Oceanogr*, 34(1): 68–81
- Carlson Craig A. 2002. Production and removal processes. *Biogeochemistry of Marine Dissolved Organic Matter*. New York: Academic Press, 91–151
- Cauwet Gustave. 2002. DOM in the Coastal Zone. In: Dennis A H, Craig A C, eds. *Biogeochemistry of Marine Dissolved Organic Matter*. San Diego: Academic Press, 579–609
- Cauwet G, Mackenzie F. 1993. Carbon inputs and distribution in estuaries of turbid rivers: the Yang Tze and Yellow rivers (China). *Marine Chemistry*, 43(1–4): 235–246
- Chen Zhiqiang, Li Yan, Pan Jianming. 2004. Distributions of colored dissolved organic matter and dissolved organic carbon in the Pearl River Estuary, China. *Continental Shelf Research*, 24(16): 1845–1856
- Chen Chu Qun, Shi Ping. 2001. Application of ocean color satellite remote sensing data for estimation of DOC concentration. *Acta Scientiae Circumstantiae*, 21(6): 5
- Dai Minhan, Meng Feifei, Tang Tiantian, et al. 2009. Excess total organic carbon in the intermediate water of the South China Sea and its export to the North Pacific. *Geochemistry Geophysics Geosystems*, 10(12): Q12002
- Del Vecchio Rossana, Blough Neil V. 2004. Spatial and seasonal distribution of chromophoric dissolved organic matter and dissolved organic carbon in the Middle Atlantic Bight. *Marine Chemistry*, 89(1–4): 169–187
- Del Castillo Carlos E, Coble Paula G, Morell Julio M, et al. 1999. Analysis of the optical properties of the Orinoco River plume by absorption and fluorescence spectroscopy. *Marine Chemistry*, 66(1–2): 35–51
- Del Castillo Carlos E, Gilbes Fernando, Coble Paula G, et al. 2000. On the dispersal of riverine colored dissolved organic matter over the west Florida shelf. *Limnol Oceanogr*, 45(6): 1425–1432
- Del Castillo C E, Miller Richard L. 2008. On the use of ocean color remote sensing to measure the transport of dissolved organic carbon by the Mississippi River plume. *Remote Sensing of Environment*, 112(3): 836–844
- Ferrari G M. 2000. The relationship between chromophoric dissolved organic matter and dissolved organic carbon in the European Atlantic coastal area and in the West Mediterranean Sea (Gulf of Lions). *Marine Chemistry*, 70(4): 339–357
- Ferrari Giovanni M, Dowell M D, Grossi S, et al. 1996. Relationship between the optical properties of chromophoric dissolved organic matter and total concentration of dissolved organic carbon in the southern Baltic Sea region. *Marine Chemistry*, 55(3–4): 299–316
- Gardner G Bernard, Chen Robert F. 2004. High-resolution measurements of chromophoric dissolved organic matter in the Mississippi and Atchafalaya River plume regions. *Marine Chemistry*, 89(1–4): 103–125
- Green Sarah A, Blough Neil V. 1994. Optical absorption and fluorescence properties of chromophoric dissolved organic matter in natural waters. *Limnol Oceanogr*, 39(8): 1903–1916
- Guo Weidong, Stedmon Colin A, Han Yuchao, et al. 2007. The conservative and non-conservative behavior of chromophoric dissolved organic matter in Chinese estuarine waters. *Marine Chemistry*, 107(3): 357–366
- Hansell Dennis A, Carlson Craig A. 2001. Marine dissolved organic matter and the carbon cycle. *Oceanography*, 14(4): 41–49
- He Biyan, Dai Minhan, Zhai Weidong, et al. 2010. Distribution, degradation and dynamics of dissolved organic carbon and its major compound classes in the Pearl River estuary, China. *Marine Chemistry*, 119(1–4): 52–64
- Hedges John I, Cowie Gregory L, Richey Jeffrey E, et al. 1994. Origins and processing of organic matter in the Amazon River as indicated by carbohydrates and amino acids. *Limnol Oceanogr*, 39(4): 743–761
- Hong Huasheng, Wu Jingyu, Shang Shaoling, et al. 2005. Absorption and fluorescence of chromophoric dissolved organic matter in the Pearl River Estuary, South China. *Marine Chemistry*, 97(1–2): 78–89
- Hung J J, Chen C H, Gong G C, et al. 2003. Distributions, stoichiometric patterns and cross-shelf exports of dissolved organic matter in the East China Sea. *Deep-Sea Research Part II: Topical Studies in Oceanography*, 50(6–7): 1127–1145
- Joos Fortunat, Plattner Gian Kasper, Stocker Thomas F, et al. 1999. Global warming and marine carbon cycle feedbacks on future atmospheric CO<sub>2</sub>. *Science*, 284(5413): 464

- Knap A, Michaels A, Close A, et al. 1996. Protocols for the joint global ocean flux study (JGOFS) core measurements. Intergovernmental Oceanographic Commission, UNESCO. 198
- Kostoglidis Antwanet, Pattiaratchi Charitha B, Hamilton David P. 2005. CDOM and its contribution to the underwater light climate of a shallow, microtidal estuary in south-western Australia. *Estuarine, Coastal and Shelf Science*, 63(4): 469–477
- Kowalczyk Piotr, Zabłocka M, Sagan Sławomir, et al. 2010. Fluorescence measured in situ as a proxy of CDOM absorption and DOC concentration in the Baltic Sea. *Oceanologia*, 52(3): 171–196
- Lei Hui, Pan Delu, Bai Yan, et al. 2012. The proportions and variations of the light absorption coefficients of major ocean color components in the East China Sea. *Acta Oceanologica Sinica*, 31(2): 45–61
- Lin Jing, Wu Ying, Zhang Jing, et al. 2007. Seasonal variation of organic carbon fluxes in the Yangtze River and influence of Three-Gorges engineering. *China Environmental Science*, 27(2): 4
- Lohrenz Steven E, Dagg Michael J, Whittedge Terry E. 1990. Enhanced primary production at the plume/oceanic interface of the Mississippi River. *Continental Shelf Research*, 10(7): 639–664
- Lohrenz Steven E, Fahnenstiel Gary L, Redalje Donald G, et al. 1999. Nutrients, irradiance, and mixing as factors regulating primary production in coastal waters impacted by the Mississippi River plume. *Continental Shelf Research*, 19(9): 1113–1141
- Lundgren B. 1976. Spectral transmittance measurements in the Baltic. Copenhagen: Copenhagen University, Institute for physical Oceanography
- Mannino Antonio, Russ Mary E, Hooker Stanford B. 2008. Algorithm development and validation for satellite-derived distributions of DOC and CDOM in the US Middle Atlantic Bight. *J Geophys Res*, 113(C7): C07051
- Mantoura R F C, Woodward E M S. 1983. Conservative behaviour of riverine dissolved organic carbon in the Severn Estuary: chemical and geochemical implications. *Geochimica et Cosmochimica Acta*, 47(7): 1293–1309
- McKee B A. 2003. RiOMar: The Transport, Transformation and Fate of Carbon in River-dominated Ocean Margins. New Orleans, LA: University T, 5–6
- Mitchell B G, Bricaud A, Carder K, et al. 2000. Determination of spectral absorption coefficients of particles, dissolved material and phytoplankton for discrete water samples. In: G Fargion and J Mueller eds. *Ocean Optics Protocols for Satellite Ocean Color Sensor Validation, Revision, 2*. Greenbelt, Md: Goddard Space Flight Center, Natl. Aeronautics and Space Admin, 125–153
- Nagata T. 2002. Production mechanisms of dissolved organic matter. In: Kirchman D L, ed. *Microbiology Ecology of the Oceans*. New York: Wiley, 121–152
- Nelson N, Siegel D, Michaels A. 1998. Seasonal dynamics of colored dissolved material in the Sargasso Sea. *Deep-Sea Research: Part I*, 45(6): 931–957
- Nieke B, Reuter R, Heuermann R, et al. 1997. Light absorption and fluorescence properties of chromophoric dissolved organic matter (CDOM), in the St Lawrence Estuary (Case 2 waters). *Continental Shelf Research*, 17(3): 235–252
- Ogawa Hiroshi, Usui Toshihiro, Koike Isao. 2003. Distribution of dissolved organic carbon in the East China Sea. *Deep-Sea Research: Part II. Topical Studies in Oceanography*, 50(2): 353–366
- Packard T, Chen W, Blasco D, et al. 2000. Dissolved organic carbon in the Gulf of St Lawrence. *Deep Sea Research: Part II. Topical Studies in Oceanography*, 47(3–4): 435–459
- Rochelle-Newall E J, Fisher T R. 2002. Chromophoric dissolved organic matter and dissolved organic carbon in Chesapeake Bay. *Marine Chemistry*, 77(1): 23–41
- Sasaki Hiroaki, Miyamura Tsuyoshi, Saitoh Sei-ichi, et al. 2005. Seasonal variation of absorption by particles and colored dissolved organic matter (CDOM) in Funka Bay, southwestern Hokkaido, Japan. *Estuarine, Coastal and Shelf Science*, 64(2–3): 447–458
- Sathyendranath S. 2000. Remote sensing of ocean colour in coastal, and other optically-complex, waters. Reports of the International Ocean-Colour Coordinating Group, No.3. Dartmouth, Canada: IOCCG P O
- Stedmon CA, Markager S. 2001. The optics of chromophoric dissolved organic matter (CDOM) in the Greenland Sea: an algorithm for differentiation between marine and terrestrially derived organic matter. *Limnol Oceanogr*, 46(8): 2087–2093
- Vodacek Anthony, Hoge Frank E, Swift Robert N, et al. 1995. The use of in situ and airborne fluorescence measurements to determine UV absorption coefficients and DOC concentrations in surface waters. *Limnol Oceanogr*, 40(2): 411–415
- Welschmeyer N A. 1994. Fluorometric analysis of chlorophyll a in the presence of chlorophyll b and pheopigments. *Limnol Oceanogr*, 39: 1985–1992
- Zhang Yun-lin, Huang Qun-fang, Ma Rong-hua, et al. 2005. Retrieving of dissolved organic carbon based on irradiance reflectance in typical lake zones of lake Taihu. *Advances in Earth Science*, 20(7): 6
- Zhu Weining, Yu Qian, Tian Yong Q, et al. 2011. Estimation of chromophoric dissolved organic matter in the Mississippi and Atchafalaya River plume regions using above-surface hyperspectral remote sensing. *J Geophys Res*, 116: C02011